Automatic Reflection Detection on Dermatological Images Acquired via Mobile Devices

Maria João M. Vasconcelos[1]
maria.vasconcelos@fraunhofer.pt
Luís Rosado[1]
luis.rosado@fraunhofer.pt

[1] Fraunhofer Portugal AICOS
Porto, Portugal

Abstract

The late detection of skin cancer, especially melanoma, leads to an increase in mortality rates, therefore it is high time to embrace mobile teledermatology and adapt the existing methodologies to check out the malignancy level of a mole. Though, the usage of a smartphone camera gives rise to new pre-processing challenges like the treatment of reflections caused by the flash light or uneven illumination conditions. In this work, a new methodology to detect reflections on mobile-acquired dermatological images is presented, based on the different behaviour in terms of highlights invariance of the L and H colour channels, from the CIE L**a***b** and HSV color spaces, respectively. The achieved results confirm the good quality of the suggested algorithm.

1 Introduction

With increasing aging population globally, there is a growing incidence of skin cancer. Nevertheless the percentage of population participating in skin cancer screening versus incidence is alarmingly low. Late detection leads to rise in skin cancer mortalities, especially melanomas, as so there is a need for complementing existing technologies in order to check out the malignancy level of a mole. In addition, given the current need to decrease the costs of the healthcare providers, the usage of new lightweight monitoring systems which can be carried around easily and used regularly by the patients, is considered crucial to find new ways of making better decisions on treatment.

Considering the high dissemination of mobile devices and their integrated image acquisition systems, mobile teledermatology appears as a promising tool for personal dermatologic data acquisition. When compared to dermoscopy [1], the current most accepted method for image acquisition in dermatology, the usage of a smartphone camera brings up a new set of challenges. Consequently, it is important to develop methodologies to deal with some of the expected artifacts like reflections, blurred images, and uneven illumination conditions. The present work focuses on the detection of reflections in dermatological images acquired via mobile devices.

The most known and commonly used color space in computer applications is the RGB (Red-Green-Blue) which are three primary additive colors and are represented by a three-

dimensional, Cartesian coordinate system. In an attempt to linearize the perceptibility of color differences, the CIE proposed two other color spaces, CIE L*u*v* and CIE L*a*b*. The HSL (hue, saturation and lightness) color space or similar ones like HSI (intensity), HSV (value) or HCI (chroma) are linear transformations from RGB. The main disadvantage of the RGB color space in applications with natural images is the high correlation between its components. The advantage of CIE absolute color spaces is that they define color exactly and thus includes more color than other color spaces, even more than the human eye can see, however they suffer from being quite unintuitive. In summary, different color spaces are better for different applications, since some colors are perceptually linear or just more intuitive to use, also some color spaces are tied to a specific equipment while other are equally valid on whatever device they are used [2].

Many different approaches to detect reflections have also been proposed over the years. One of the most popular model is the dichromatic reflection model proposed by Shafer 1985 [3], it separates reflectance into surface body reflectance and interface reflectance. However the application of this model to uncalibrated real-word images led to multiple problems. In [4] an overview of the methods to separate reflection components, also known as specularity or highlights removal is given. In [5] the authors use a simple reflection detection algorithm that applies thresholds to the intensity and the difference between the intensity and the average intensity; however it is applied only to dermoscopy images. In [6], the authors introduces a low-level feature for recognizing reflective objects from natural images, also showing how to characterize static specular flows and identify specular surfaces with minimal requirements about the illumination conditions and utilizing a single monocular image.

Recently, [7] presented an automated technique for detecting reflections in image sequences through the analysis of motion trajectories of feature points. In [8] an algorithm for reflections removal specifically for images acquired from mobile phones is presented, however it requires the user to take two pictures, one with flash light and another without in order to produce the new picture with the reflections removed.

The structure of this paper is as follows: the next section describes the dataset used in this work; section 3 details the methodology to detect reflections for dermatological images; section 4 presents and discusses the obtained results; to end, conclusions and future work are summarized.

2 Dataset

The database used in our study was obtained under the scope of the Melanoma Detection, a project that intends to create a prototype for a patient-oriented system of skin lesion analysis using a smartphone [9]. The database contains a total of 90 images, 8-bit color with 652x652 pixels of resolution acquired with a mobile phone Htc One S.

Each image of this dataset was later labelled by 5 subjects regarding its reflection level, using a scale from 0 to 3. Subjects were asked to label each image taking only into consideration the mole area, being supplied a complete image and another only with the segmented mole. The final dataset was classified according the most voted class and the images with less than 3 equal votes were discarded from the study. A final dataset of 75 images were used to validate our algorithm, where 16 images were classified with no reflections (class 0), 27 with few reflections (class 1), 22 with some reflections (class 2) and 10 with many reflections (class 3).

3 Reflection Detection Algorithm

The first step of this algorithm consists in applying a retina Parvo filtering [10], where the mean luminance is attenuated, the spectrum is whitened and the contours enhanced. The retina model takes into account the processing occurring at the retina level, being developed to prepare images for high level processing and designed to be used in contexts where contours and contrasts constitute important information, which is our case.

Afterwards, the filtered RGB image is transformed into Lab color space to obtain L channel according to equations (1) and (2):

$$\begin{bmatrix} X \\ Y \\ Z \end{bmatrix} = \begin{bmatrix} 0.412453 & 0.357580 & 0.180423 \\ 0.212671 & 0.715160 & 0.072169 \\ 0.019334 & 0.119193 & 0.950227 \end{bmatrix} \cdot \begin{bmatrix} R \\ G \\ B \end{bmatrix}, \tag{1}$$

$$L = \begin{cases} 116 * Y^{1/3} - 16 & for \quad Y > 0.008856 \\ 903.3 * Y & for \quad Y \leq 0.008856 \end{cases}. \tag{2}$$

As the studies indicate [2], the H channel is invariant to highlights so we inferred if this condition was still preserved for dermatological images. The previous statement was confirmed in our study nonetheless, after some further exploration on the H channel original equation, our research indicated that the inclusion of slight variation on it brought significant better results concerning highlights invariance. Therefore, the H* channel is calculated from the HLS space taking into consideration the subsequent equation (3):

$$H^* = 60(G - B)/(\max(R, G, B) - \min(R, G, B)) \tag{3}$$

Because $0 \leq H^* \leq 360$, the channel is later normalized to fit between 0 and 1 and be comparable to the L channel. Taking into account that the L channel is considered dependent on highlights, while the H channel is invariant to highlights [2], the difference between the L and H* channel is obtained with the purpose of investigate if it enhanced the reflection regions. And in fact, the results attained with the difference mask were better than the ones using only the H* channel, so we decided to choose for the first option.

In order to remove small artifacts on the differences mask, the image is then smoothed using a Gaussian filter. Median filter and average filter were also tested to smooth the differences mask and turned to be less effective. This can be explained by the fact that neighbor pixels in Gaussian filter have different coefficients related with Gaussian distribution, having the current pixel a more significant contribution. Thus the edges are more preserved in Gaussian filtering, which in our case are the reflections.

Finally, to segment reflection regions, the histogram of the difference mask is computed and the color level with maximum frequency is chosen as the binarization threshold. This threshold is appropriate independently of the fact that the maximum frequency represents the background or the skin mole groups, because the color variation of the background and skin mole pixel groups is lower after Gaussian filtering, and also only reflections inside the mole segmentation mask are considered.

Figure 1 depicts the outputs along the several steps of our algorithm: first we present the original image, followed by the image after the application of the retina filter, then images of the L and H channels are portrait as well as the resulting difference, after that the segmentation of the mole is shown (in white) and the mask of reflections (in black), at last we represent the final mask.

The algorithm was developed using C++ and OpenCV library [11]. To quantify the presence of reflection regions in each image, the relative area of the obtained reflection mask was calculated, by dividing the area of the reflection zones by the total area of each mole. The total area of the skin mole corresponds to the area of the correspondent segmentation mask, which was obtained using a simple adaptive segmentation method [12]. In addition, the number of blobs on each reflection mask was also calculated.

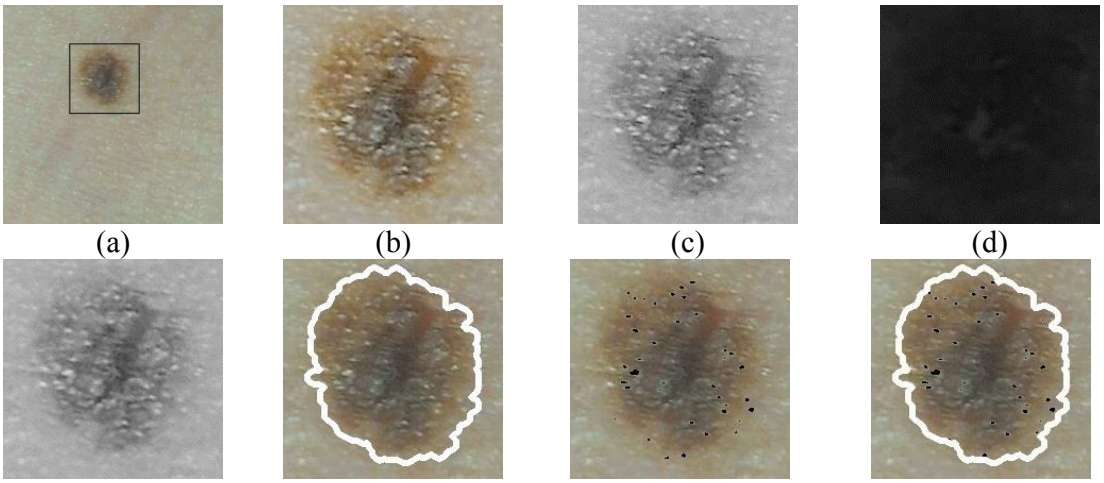

Figure 1: Example of results obtained during the application of the reflection algorithm: (a) original image; (b) after using the retina filter; (c and d) L and H* channels; (e) difference mask; (f) segmentation mask in white; (g) reflection mask in black; (h) final mask.

4 Results

In this section we present the results of the proposed algorithm, using the previously referred image dataset. As it was previously said, the images on the used dataset were classified according to its level of reflections. Figure 2 portrays examples of images of each category in the first row and the second row the reflection mask result is presented. From that, the one could confirm that the suggested algorithm shows a promising discriminatory ability for reflection regions; images classified with no or few reflections present reflection masks with a significant lower occurrence of reflection regions, when compared with images classified as having some or many reflections. To ensure the quality of the presented algorithm, besides the visual inspection, the authors calculated the relative area of the obtained reflection mask in addition to the number of blobs. Figure 3 depicts the distribution graphs for each class of images that once again confirm our methodology. Clearly, as the classes advance in terms of the incidence of reflections, the values of relative area and number of blobs arise.

However for class 1 a high maximum was obtained for the relative area and for class 2 the same occurs for the maximum number of blobs. So, we have decided to look the corresponding images in more detail, which can be observed in figure 4. The first image was classified has having few reflections, in fact 3 subjects classified it as having few reflections and the other 2 subjects classified it as class 2, by looking at the original image it is fair to consider that this image was misclassified. The same happens with the other outlier of class 2, the image was classified as class 2 with 3 votes, and the other subjects voted class 3, this image should be considered as class 3.

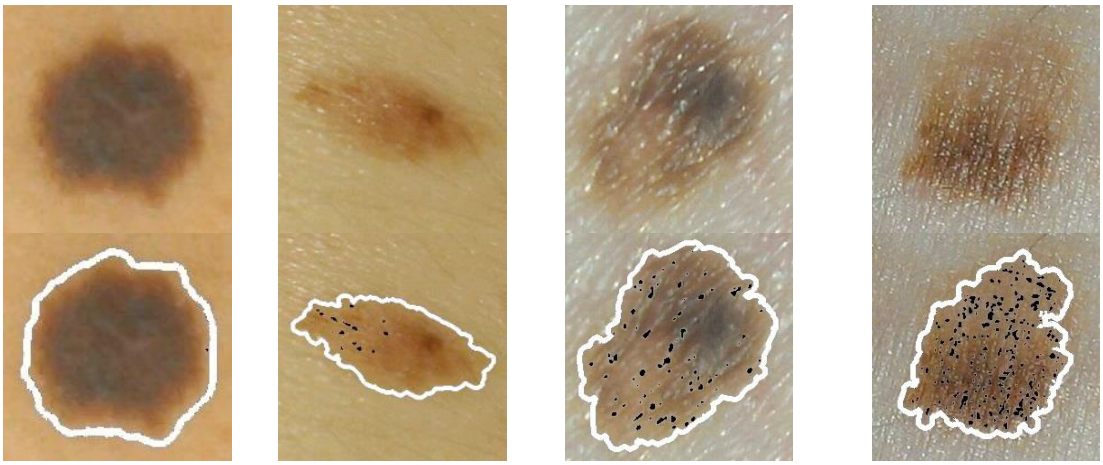

No reflections (0) Few reflections (1) Some reflections (2) Many reflections (3)

Figure 2: Examples of original images (first row) and resulting reflection detection masks (second row) for each class.

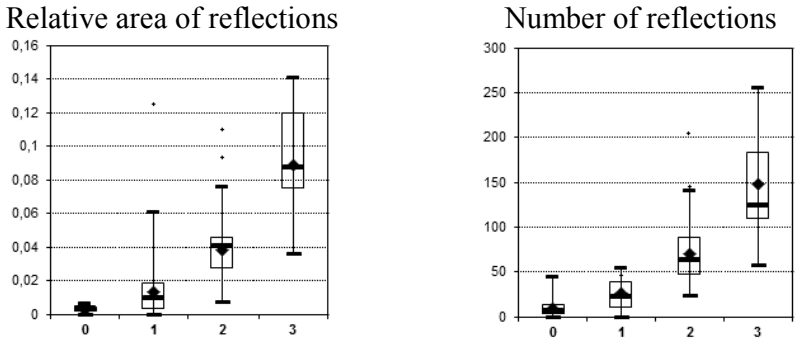

Figure 3: Data distribution for relative area and number of reflections (vertical axis) for each class (horizontal axis).

Figure 4: Images and resulting reflection detection mask of two outliers identified from the data distribution charts.

5 Conclusions and Future Work

The development of algorithms for pre-processing analysis especially designed for application in dermatological images acquired from mobile devices is definitely a requisite nowadays. Algorithms capable of doing image quality assessment for these specific images are of extreme importance to ensure that images analysis obtains proper results.

In this work we explore an algorithm to detect deteriorated zones due to reflection in dermatological images, either caused by the flash light or uneven illumination conditions. The presented methodology proved to be capable of performing such task. As far as we know this is the first study that performs the pre-processing of dermatological single images captured via mobile phone orientated to the skin cancer prevention.

As future work we intend to expand this study by augmenting the datasets, using images from different mobile phone brands as well as explore the suitability of this algorithm to general macroscopic images. The methodology of classifying the reflection should also be improved, for instance with the inclusion of more subjects in the classification or searching for alternative methods to generate a ground truth dataset.

Acknowledgements

This work was done under the scope of the project "SMARTSKINS: A Novel Framework for Supervised Mobile Assessment and Risk Triage of Skin Lesion via Non-invasive Screening" with reference PTDC/BBB-BMD/3088/2012 financially supported by Fundação para a Ciência e a Tecnologia in Portugal. The authors would also like to thank the cooperation of the researchers Liliana Ferreira, Filipe Soares, Vânia Guimarães and David Ribeiro in images classification.

References

[1] H. Kittler, H. Pehamberger and K. Wolff. Binder M.: Diagnostic accuracy of dermoscopy. Lancet Oncol., 3(3):159-165, 2002.

[2] T. Gevers, A. Gijsenij, J. van de Weijer and J-M Geusebroek. Color in Computer Vision: Fundamentals and Applications. Wiley, 2012.

[3] S. Shafer. Using color to separate reflection components. COLOR research and application, 10(4):210–218, 1985.

[4] A. Artusi, F. Banterle and D. Chetverikov. A survey of specularity removal methods. *Computer Graphics Forum*, 30 (8): 2208-2230, Blackwell Publishing Ltd, 2011.

[5] C. Barata, J. S. Marques and J. Rozeira. Detecting the pigment network in dermoscopy images: a directional approach. *Engineering in Medicine and Biology Society, EMBC, 2011 Annual International Conference of the IEEE*: 5120-5123, IEEE, 2011

[6] A. DelPozo and S. Savarese. Detecting specular surfaces on natural images. *Computer Vision and Pattern Recognition, 2007, IEEE Conference on:* 1-8, IEEE, 2007.

[7] M. A. Ahmed, F. Pitie and A. Kokaram. Reflection detection in image sequences. *Computer Vision and Pattern Recognition (CVPR), 2011 IEEE Conference on*: 705-712, IEEE, 2011.

[8] Y. Geng and Z. Jian. Reflections Removal on Mobile Devices. Project Report Stanford University, Digital Image Processing, 2013.

[9] Fraunhofer Portugal AICOS. Melanoma Detection. Internal Project, http://www.fraunhofer.pt/en/fraunhofer_aicos/projects/internal_research/melanoma_detection.html

[10] A. Benoit, A. Caplier, B. Durette and J. Herault. Using Human Visual System Modeling For Bio-Inspired Low Level Image Processing. Computer Vision and Image Understanding, 114: 758-773, Elsevier, 2010.

[11] G. Bradski and A. Kaehler. Learning OpenCV: Computer Vision with the OpenCV Library, O'Reilly Media Inc., 2008.

[12] L. Rosado, M.J. Vasconcelos and M. Ferreira. A Mobile-Based Prototype for Skin Lesion Analysis: Towards a Patient-Oriented Design Approach. *International Journal of Online Engineering* (iJOE), dec 27-29, 2013.